A Least-Squares Estimation Approach to Improving the Precision of Inverse Dynamics Computations

A. D. Kuo
Department of Mechanical Engineering & Applied Mechanics,
University of Michigan,
Ann Arbor, MI 48109

A least-squares approach to computing inverse dynamics is proposed. The method utilizes equations of motion for a multi-segment body, incorporating terms for ground reaction forces and torques. The resulting system is overdetermined at each point in time, because kinematic and force measurements outnumber unknown torques, and may be solved using weighted least squares to yield estimates of the joint torques and joint angular accelerations that best match measured data. An error analysis makes it possible to predict error magnitudes for both conventional and least-squares methods. A modification of the method also makes it possible to reject constant biases such as those arising from misalignment of force plate and kinematic measurement reference frames. A benchmark case is presented, which demonstrates reductions in joint torque errors on the order of 30 percent compared to the conventional Newton–Euler method, for a wide range of noise levels on measured data. The advantages over the Newton–Euler method include making best use of all available measurements, ability to function when less than a full complement of ground reaction forces is measured, suppression of residual torques acting on the top-most body segment, and the rejection of constant biases in data.

Introduction

Inverse dynamics, the procedure in which motion data are used to estimate torques (i.e., moments of muscle force) produced at the joints, is a primary tool for analysis of gait and other movements. It is a simple and effective technique, which can be used to infer which and how muscles are used in a motor task. A variety of data are needed to make the necessary calculations, including anthropometric parameters specifying the inertial properties of each limb, a record of the limb movements, and often, a record of ground reaction forces. Because these data are not generally known precisely—and in the cases of limb kinematics and ground reaction forces, their precision often comes at considerable expense—it is usually desirable to extract the best possible joint torque estimates from imperfect measurements.

The conventional method for computing inverse dynamics is quite simple (Winter, 1990). A typical scheme involves iterative solution of the Newton–Euler equations of motion for each body segment. If only angular acceleration measurements are available, the iteration starts at the top-most segment, calculating joint torques that satisfy dynamic equilibrium conditions at each successive segment proceeding downward. This method tends to produce noisy joint torque estimates, because angular accelerations are typically determined by twice-differentiating motion data with respect to time, and the differentiation process tends to amplify measurement noise. A modification of this scheme is to introduce additional measurements in the form of ground reaction forces. These data provide boundary conditions for the bottom-most segment, and the dynamic equilibrium conditions are applied at each successive segment proceeding upward. Because force plate data are typically less noisy than acceleration data, the resulting joint torque estimates tend to be more precise. However, the introduction of additional data provides more equilibrium conditions than can be satisfied. This overdeterminacy may be avoided by either discarding the acceleration measurements for the top-most segment, or by adding residual forces and torques to the top-most segment.

There are alternative formulations for the inverse dynamics problem, which are based on optimization. Vaughan et al. (1982) noted the overdeterminacy arising from introduction of ground reaction forces, and proposed using the extra degrees of freedom to optimize the body segment parameters. This method indirectly improves inverse dynamics computations by providing better parameter values and enforcing the boundary conditions, but does not otherwise affect the joint torque estimates. Perhaps the most sophisticated approach is to use dynamic optimization to compute the trajectory of joint torques, which in a forward simulation best reproduces the observed motion (Chao and Rim, 1973). This method enforces the dynamic equations of motion over time, and thus may be regarded as a theoretically ideal method for estimating joint torques.

There are, however, several disadvantages to both conventional and dynamic optimization methods for computing inverse dynamics. In the presence of noise, the conventional Newton–Euler method produces poor joint torque estimates when ground reaction forces are not measured, and produces a residual when they are. It is also highly sensitive to mismatch in the origins of reference frames for motion data and ground reaction forces (McCaw and DeVita, 1995). Dynamic optimization can be used to overcome some of these problems, but practical experience with this method shows that it is often difficult to find a solution, or even the initial guess at a solution that is required to start the optimization. The dynamics of a standing or walking human are inherently unstable, and so virtually any initial guess will diverge within a certain number of time constants for the system. An initial guess will only work for unstable systems if it is exceedingly accurate, or if the time period of the analysis is too short to allow for divergence. For example, Chao and Rim (1973) demonstrated the use of dynamic optimization for 0.17

Contributed by the Bioengineering Division for publication in the JOURNAL OF BIOMECHANICAL ENGINEERING. Manuscript received by the Bioengineering Division January 10, 1996; revised manuscript received March 5, 1997. Associate Technical Editor: A. G. Erdman.

 Copyright © 1998 by ASME

of mass with Cartesian coordinates in the plane described by a two-component vector x_{ci}, and a scalar orientation in spatial coordinates ϕ_i. Knowledge of ϕ_i for $i = 1, 2, \ldots n$ is sufficient to fully determine the configuration of the system, including x_{ci}, and so the ϕ_i may be regarded as generalized coordinates (Greenwood, 1988). The joints between segments are numbered from 1 to $n - 1$, with joint i articulating segments i and $i + 1$. There are intersegmental forces f_{i-1} (with 2 components) acting on the end of segment i corresponding to joint $i - 1$, and $-f_i$ acting at the end corresponding to joint i. Similarly there are joint torques τ_{i-1} and $-\tau_i$ acting on the same respective ends. The ground reaction forces and torques are f_0 and τ_0, respectively, and so the force plate may be regarded as segment $i = 0$. The following quantities will be also stacked together and referred to in vector form:

$$\phi \equiv \begin{bmatrix} \phi_2 \\ \phi_3 \\ \vdots \\ \phi_n \end{bmatrix}, \quad \tau \equiv \begin{bmatrix} \tau_1 \\ \tau_2 \\ \vdots \\ \tau_{n-1} \end{bmatrix}.$$

It will be convenient to recognize the difference between a quantity's actual value denoted by a horizontal bar (e.g., $\bar{z}$), its measured value denoted by a prime (z'), and its estimated value (which does not generally equal the measured value) denoted by the unadorned symbol (z). The errors in measurement arise from additive noise:

$$\phi' = \bar{\phi} + w_\phi$$

$$f_0' = \bar{f}_0 + w_{f0}$$

$$\tau_0' = \bar{\tau}_0 + w_{\tau 0}$$

where w_ϕ, w_{f0}, and $w_{\tau 0}$ are white noise vectors, which are assumed to have Gaussian distribution with zero mean.

Angular acceleration measurements $\ddot{\phi}'$ are found by twice-differentiating the angular orientations,

$$\ddot{\phi}' = \ddot{\bar{\phi}} + w_{\ddot{\phi}}$$

where $w_{\ddot{\phi}}$ is the (nonwhite) acceleration noise. The process of numerical differentiation tends to amplify noise, so that velocity and angular orientation measurements have relatively small errors relative to the acceleration measurements. Hence, the estimates of angular orientation and velocity will be set equal to their measurements, $\phi = \phi'$ and $\dot{\phi} = \dot{\phi}'$ (ϕ_1 is assumed constant).

Conventional Newton–Euler Method. Conventional inverse dynamics methods compute the intersegmental reaction forces using Newton's equation of motion and Euler's equation, applied to each of the segments at each point in time:

$$m_i I^{2\times 2} \ddot{x}_{ci} = f_{i-1} - f_i \tag{1}$$

$$I_i \ddot{\phi}_i = r_i \times f_{i-1} - s_i \times f_i + \tau_{i-1} - \tau_i \tag{2}$$

where m_i is the mass, $I^{2\times 2}$ is the two-by-two identity matrix, and $\ddot{x}_{ci}$ is the translational acceleration vector as described previously; I_i is the moment of inertia, and r_i and s_i are vectors from the center of mass to the joints at the bottom-most and top-most ends, respectively, of segment i.

Consider first an inverse dynamics problem in which there are no ground reaction forces measured. The estimated joint angular accelerations are set equal to their measured values, $\ddot{\phi}_i = \ddot{\phi}_i'$, $i = 2, \ldots, n$, with the assumption $\ddot{\phi}_1 = 0$. The problem may be solved iteratively by setting boundary conditions on the top-most segment, $f_n = 0$ and $\tau_n = 0$, and applying dynamic equilibrium, Eqs. (1) and (2), to calculate the forces and torques acting at the other end of the segment. This procedure is repeated for each segment from n to 1, solving for each joint torque successively.

When ground reaction forces and torque are measured, they may be included by using them as boundary conditions on the bottom-most segment, $f_0 = f_0'$, $\tau_0 = \tau_0'$, and applying dynamic equilibrium on each segment proceeding upward. Equations (1) and (2) are employed starting at $i = 1$, with $\ddot{\phi}_i = \ddot{\phi}_i'$. The extra force inputs act as additional constraints on the equations, making the system overdetermined. This difficulty is typically circumvented by introducing new degrees of freedom at the opposite end of the body, in the form of residual forces and torques at the topmost segment, f_n and τ_n, as illustrated in Fig. 1. When the measurements are imperfect, the boundary conditions $f_n = 0$, $\tau_n = 0$ are generally violated.

Although the precision of the computation is often improved by the inclusion of ground reaction forces and torques, which are typically more precise than acceleration measurements, there are several disadvantages to the methods outlined above. First, a (generally nonzero) residual is produced for each force measurement introduced, in direct contradiction of the known boundary conditions. Second, the results are often poor when acceleration measurements are noisy, especially if less than a full complement of the measurements f_0' and τ_0' is available. In addition, errors in alignment of force plate and motion analysis coordinates can result in significant errors in the joint torque estimates (McCaw and DeVita, 1995).

Proposed Least-Squares Method. An alternative method is to solve the overcomplete system of equations without relaxing the boundary conditions. Rather, the constraints formed by imperfect measurements are relaxed by some amount so that there is a set of joint torques that satisfies a new set of adjusted measurement constraints. The criterion for choosing the joint torques is to minimize the adjustments necessary to make the measurement constraints agree with each other. This has the effect of canceling out random error in the measurements, thereby improving the precision of joint torque estimates. The method is essentially a static optimization problem formulated in matrix form and solved using the pseudoinverse. The ground reaction forces and angular accelerations are the measurements to be adjusted, and the joint torques are the variables to be estimated. (The intersegmental joint reaction forces f_i for $i = 2, \ldots, n$ need not be estimated directly as in the conventional methods, because they are noncontributory and can be found from the estimated joint torques.)

Two sets of equations are necessary to set up the overcomplete system. The first is the equations of motion relating joint torques and angular accelerations, expressed in the form

$$M(\phi)\ddot{\phi} = Q \cdot \tau + g(\phi) + v(\phi, \dot{\phi}) \tag{3}$$

where M is the mass matrix, Q is a matrix converting joint torques to segment torques, and g and v are vectors containing gravitational terms and velocity-dependent terms, respectively (see Appendix A). The second set relates joint torques to the other measurements, the ground reaction forces. It can be found by first deriving the body equations of motion including additional degrees of freedom for motion of segment $i = 1$. These equations are used to find the constraint forces necessary to keep that segment motionless, which are identical to the ground reaction forces. The result is an equation that is linear in $\ddot{\phi}$,

$$C(\phi)\ddot{\phi} = \begin{bmatrix} \tau_0 \\ f_0 \end{bmatrix} + c(\phi, \dot{\phi}) \tag{4}$$

where $C(\phi)$ is an intermediate term relating angular accelerations and reaction forces (see Appendix A). Equation (3) is then used to replace $\ddot{\phi}$ in Eq. (4), resulting in the desired relation,

$$C(\phi) \cdot M^{-1}(\phi) \cdot Q \cdot \tau = \begin{bmatrix} \tau_0 \\ f_0 \end{bmatrix} + c(\phi, \dot{\phi}) - C(\phi) \cdot M^{-1}(\phi) \cdot \{g(\phi) + v(\phi, \dot{\phi})\}. \tag{5}$$

s of a step in human gait. Even when a suitable initial guess is found, the iterative methods for finding the optimal solution pose a heavy computational burden.

An alternative to these methods is to treat the inverse dynamics problem as an overcomplete system of equations, and use static optimization to find the set of joint torques that agrees best with available measurements, at each point in time. The resulting torques are theoretically not as precise as those found using dynamic optimization, because (as in the conventional method) the dynamic equations of motion are not enforced over time. However, the static optimization approach is far easier and faster to solve, and has several advantages over the more widely used conventional method. First, the static optimization method makes best use of all available data, with the effect of rejecting random noise in the measurements. Second, it produces joint torque estimates, which are fully consistent with the equations of motion at each point in time, without producing residual forces and torques. Third, the proposed method works well even without a full complement of ground reaction data. And finally, the method can be extended to correct for mismatch between reference frames for ground reaction and motion data, thereby removing some biases in the joint torque estimates. Portions of this work have been introduced elsewhere (Kuo, 1994, 1995).

This paper outlines the use of static optimization to solve the inverse dynamics problem. It discusses both the overdeterminacy in the conventional method, and the use of least-squares optimization as an alternative way to estimate the joint torques. Estimation theory is used to provide predictions of error statistics for both methods. A simulated postural motion, for which exact joint torques are known, is used to compare performance and to test the error predictions. An alternative formulation is also given for the purpose of eliminating the effects of measurement bias.

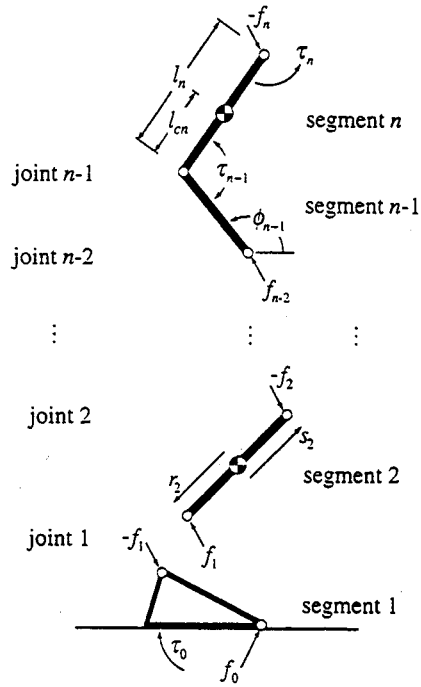

Fig. 1 Configuration of two-dimensional body segment model. The body consists of n segments, connected by n-1 joints. A joint torque τ_i and an intersegmental reaction force f_i act on the two segments (but with opposite signs) connected by joint i. The angular orientation of each segment is given by ϕ_i. Vectors r_i and s_i are from segment i's center of mass to the joints. Segment length and location of center of mass are specified by l_i and l_{ci}. The force and torque vectors shown illustrate points of application and do not imply specific directions. Sign conventions and angular reference are also arbitrary, but are defined here such that joint torques are positive in extension and angular orientations are measured counterclockwise from the horizontal.

Method

The proposed method differs from the conventional Newton–Euler method in a fundamental way. The conventional method treats each body segment separately, applying dynamic equilibrium conditions to compute all intersegmental forces and torques. The proposed method uses equations of motion based on generalized coordinates to treat all segments simultaneously, thereby relating joint torques to angular accelerations without need for intersegmental forces. Another set of equations relates joint torques to the ground reaction forces. These two sets of equations are linear in the joint torques, and form an overcomplete system, which can be solved analytically using a simple least-squares pseudoinverse, providing the optimal solution that agrees best with the measurements. The problem is formulated stochastically using estimation theory, to take into account noise in the measurements and provide a prediction of the error covariance. An alternate formulation produces a sparse overdetermined system, which can be used to eliminate biases arising from misalignment of force/motion data or other causes. For simplicity, the derivations and accompanying test case are performed for a two-dimensional system. The method, however, is fully applicable to three-dimensional systems with appropriate changes described in Appendix C.

The following nomenclature will be adopted for the general two-dimensional system, as shown in Fig. 1. The body comprises n segments, of which one, typically the foot, remains motionless in static contact with a force plate. These segments are numbered $i = 1, 2, \ldots n$, starting with the motionless segment and moving successively to other segments, which are more distal from the force plate. Each segment i has a center

Nomenclature

n = number of body segments
N = number of time steps
$\bar{x}_{ci}$ = vector describing linear (translational) position of segment i's center of mass
x_{ci}, x'_{ci} = estimated and measured values of $\bar{x}_{ci}$
$\bar{\dot{x}}_{ci}, \dot{x}_{ci}, \dot{x}'_{ci}$ = actual, estimated, and measured linear velocity vectors
$\bar{\ddot{x}}_{ci}, \ddot{x}_{ci}, \ddot{x}'_{ci}$ = actual, estimated, and measured linear acceleration vectors
$\bar{\phi}_i$ = actual angular orientation of segment i (segment angle)
ϕ_i, ϕ'_i = estimated and measured values of $\bar{\phi}_i$
$\bar{\dot{\phi}}_i, \dot{\phi}_i, \dot{\phi}'_i$ = actual, estimated, and measured angular velocity vectors
$\bar{\ddot{\phi}}_i, \ddot{\phi}_i, \ddot{\phi}'_i$ = actual, estimated, and measured angular acceleration vectors
$\bar{f}_{i-1}$ = intersegmental reaction force vector acting on segment i at joint $i-1$
f_i, f'_i = estimated and measured values of $\bar{f}_i$
$\bar{\tau}_{i-1}$ = actual joint torque (moment of muscle force) applied on segment i at joint $i-1$
τ_i, τ'_i = estimated and measured values of $\bar{\tau}_i$
f_0, τ_0 = estimated ground reaction forces and torque
$w_{f0}, w_{\tau 0}, w_\phi$ = measurement noise in f'_0, τ'_0, ϕ'

which is linear in τ. The full derivation for the benchmark system, as well as definitions of the relevant terms, are given in Appendix A.

The overdetermined system of equations is formed by combining Eqs. (3) and (5) and substituting measurements for ground reaction forces and torques and angular accelerations into the right-hand side:

$$\begin{bmatrix} C(\phi)\cdot M^{-1}(\phi)\cdot Q \\ M^{-1}(\phi) \end{bmatrix}\cdot\tau = \begin{bmatrix} \tau_0' \\ f_0' \\ \ddot{\phi}' \end{bmatrix} + \begin{bmatrix} c(\phi,\dot{\phi}) \\ \cdots\cdots \\ 0 \end{bmatrix} - \begin{bmatrix} C(\phi) \\ I^{n\times n} \end{bmatrix}\cdot M^{-1}(\phi)\cdot\{g(\phi)+v(\phi,\dot{\phi})\}. \quad (6a)$$

It is preferable to define new variables to put Eq. (6a) into a simpler form:

$$A \equiv \begin{bmatrix} C(\phi)\cdot M^{-1}(\phi)\cdot Q \\ M^{-1}(\phi) \end{bmatrix},$$

$$b \equiv \begin{bmatrix} \tau_0' \\ f_0' \\ \ddot{\phi}' \end{bmatrix} + \begin{bmatrix} c(\phi,\ddot{\phi}) \\ \cdots\cdots \\ 0 \end{bmatrix} - \begin{bmatrix} C(\phi) \\ I^{n\times n} \end{bmatrix}\cdot M^{-1}(\phi)\cdot\{g(\phi)+v(\phi,\dot{\phi})\}$$

The linear, overdetermined nature of Eq. (6a) then becomes more evident:

$$A\cdot\tau = b, \quad (6b)$$

where the number of rows in A and b exceeds that of τ by the number of ground reaction measurements. There is in general no solution to this equation if the measurements are noisy.

Static optimization may be used to find the joint torques τ which (in the least-squares sense) best agree with the measurements:

$$\tau = \arg\min_{\tau} \|A\cdot\tau - b\|^2 \quad (7)$$

where the norm of a vector of length m is defined by $\|x\|^2 \equiv (1/m)\sum_{j=1}^{m} x_j^2$, and arg min refers to the value of τ that minimizes the norm. The linear form of Eq. (6b) is convenient because it affords a linear solution using the pseudo-inverse (Strang, 1988). While the solution to Eq. (7) is straightforward to find deterministically, it is advantageous to use a stochastic formulation based on estimation theory, because it facilitates a statistical description of the expected errors (Stark and Woods, 1986). Assume that the covariance of the (zero-mean) measurement errors is given by W:

$$E\left[\left(\begin{bmatrix} \tau_0' \\ f_0' \\ \ddot{\phi}' \end{bmatrix} - \begin{bmatrix} \bar{\tau}_0 \\ \bar{f}_0 \\ \bar{\ddot{\phi}} \end{bmatrix}\right)\cdot\left(\begin{bmatrix} \tau_0' \\ f_0' \\ \ddot{\phi}' \end{bmatrix} - \begin{bmatrix} \bar{\tau}_0 \\ \bar{f}_0 \\ \bar{\ddot{\phi}} \end{bmatrix}\right)^T\right] = W.$$

If all of the measurement errors are independent, then W is a diagonal matrix containing the variances of the measurements. The optimal estimate τ is given analytically by

$$\tau = (A^T\cdot W^{-1}\cdot A)^{-1}\cdot A^T\cdot W^{-1}\cdot b \quad (8)$$

in which the weighted pseudo-inverse of the left-hand matrix multiplier of Eq. (6b) is multiplied against the measurements. This estimate is optimal in the sense that it is the unbiased (i.e., $E[\tau] = \bar{\tau}$) linear estimator that minimizes the covariance of the estimation error, $E[(\tau - \bar{\tau})(\tau - \bar{\tau})^T]$.

Besides providing an estimate that is fully consistent with the boundary conditions and has minimum error covariance, this formulation is well suited to situations in which not all measurements are available. If any measurement from $\ddot{\phi}'$, f_0', τ_0' is unavailable or unreliable, the corresponding terms in the covariance matrix W may be set to infinity (or equivalently the corresponding terms in W^{-1} are set to zero), which has the effect of removing measurements from the equations. As long as the remaining rows of Eq. (8) are well-conditioned and of sufficient rank, the method provides an optimal estimate.

There are two practical issues to consider when implementing the solution of Eq. (8). First, it is generally computationally advantageous to use a method such as singular value decomposition to solve Eq. (6), rather than to compute the pseudo-inverse explicitly (Golub and Van Loan, 1989). Second, it is possible in some cases that the scaling that occurs with use of the covariance W may make the equation ill-conditioned. Such a situation may arise when several of the measurements are so poor that there is effectively not enough information to determine the solution fully. This may be monitored by examining the condition number of the term multiplying b in Eq. (8)—if it becomes ill-conditioned, it is preferable to scale W to keep the condition number under a reasonable value, such as 100. Fortunately, this situation rarely occurs in practice, as most measurements are usually within a few orders of magnitude of each other in precision.

Correction of Measurement Bias. The proposed least-squares estimation method can be modified to eliminate measurement biases that are constant in time, by including these biases as estimation variables, and performing the estimation across all points in time simultaneously. The simplest form of a bias is a constant offset in some of the forces, as may occur when load cells drift slowly over time. But constant biases may also be introduced by mismatch between certain estimated anthropometric parameters used to model a subject and their actual values. For example, an improper body mass estimate will produce a constant error in ground reaction torque equal to the error in units of weight multiplied by the moment arm about the force plate's coordinate origin. Another means by which constant error may be introduced is in the moment arm itself, as may occur with misalignment between force plate and motion analysis system.

Biases may be included in the estimation problem as follows: Let there be n_b unknown biases assembled into a vector β. These offsets are included by modifying Eq. (6b):

$$A[k]\tau[k] = b[k] + B\cdot\beta \quad (9)$$

where the brackets $[k]$ denote evaluation of the quantities at time k, with a total of N time steps. A selection matrix B is multiplied against β so that the biases affect the appropriate measurements. B is defined to be of size $n_m \times n_b$ where n_m is the number of measurements (or the length of $b[k]$), and to have entries $B_{ij} = 1$ if bias j acts on measurement i, $B_{ij} = 0$ otherwise.

Equation (9) may be solved for all $\tau[k]$ and β simultaneously by combining all time steps into a block linear system:

$$\begin{bmatrix} A[1] & & & & -B \\ & A[2] & & & -B \\ & & \ddots & & -B \\ & & & A[N] & -B \end{bmatrix}\begin{bmatrix} \tau[1] \\ \tau[2] \\ \vdots \\ \tau[N] \\ \beta \end{bmatrix} = \begin{bmatrix} b[1] \\ b[2] \\ \vdots \\ b[N] \end{bmatrix} \quad (10)$$

The resulting system, with size n_m by $(n\cdot N + n_b)$, is considerably larger than the single $A[k]$ of Eq. (9). It may, however,

be solved efficiently using algorithms tuned for sparse systems (Golub and Van Loan, 1989).

Error Analysis. The tools of estimation theory provide a prediction of the errors arising from each of the methods described above. For the conventional method, the prediction is made by first assembling Eqs. (1) and (2) for each segment together into a matrix equation of the form (see Appendix A)

$$\tau = F \cdot \begin{bmatrix} \ddot{\phi}' \\ \tau_0' \\ f_0' \end{bmatrix} + \gamma. \tag{11}$$

The covariance of torque estimate error using the Newton–Euler method is given by

$$X_{NE} = F \cdot W \cdot F^T. \tag{12}$$

Similarly, the error covariance for the least-squares method is given by

$$X_{LS} = (A^T W^{-1} A)^{-1} = A^{\#} W A^{\#^T} \tag{13}$$

where $A^{\#}$ denotes the pseudoinverse of A, $A^{\#} \equiv (A^T A)^{-1} A^T$. The predicted variance for the joint torque errors is given by the diagonals of X_{LS}. Assuming that the measurement noise has zero mean, the joint torque estimation errors using either method will also have zero mean.

"Experimental" Comparison of Methods. A simulated experiment was performed to compare the least-squares and Newton–Euler methods of estimating joint torques. While actual joint torques are never known exactly in a real experiment, a simulation provides the means to test performance objectively and evaluate the accuracy of the error covariance prediction. The benchmark case modeled postural sway of a four-segment body in the sagittal plane. Ground reaction forces (horizontal and vertical force and reaction torque) and the kinematics of markers located at the joint centers were calculated and then "measured" by adding zero mean white noise with known variance. These data were sampled at 60 Hz, and both forces and angular orientations derived from the marker positions were low-pass filtered with a cutoff of 5 Hz (Butterworth, third order, forward and backward passes). First and second derivatives of the filtered angular orientations were found using second-order finite differences. Equations of motion and parameters for the model are given in Appendix A. This example is not typical of all possible experiments, but is used to illustrate a single application of the least-squares method.

The simulated motion consisted of 4 seconds of a postural movement about the ankle, knee, and hip joints. The movement was produced by a feedforward trajectory of joint torques equal to the sum of sinusoids ranging from 0.5 to 2.2 Hz, plus a feedback component designed to ensure stability of the system. The amplitudes of the sinusoids were set at physiologically plausible values, and their respective phases were randomly assigned (see Fig. 2).

Four sets of simulations were performed, using varying amounts of measurement noise. For each case, the measurement noise covariance was computed and used as input to Eq. (8). Trials using both the Newton–Euler and least-squares methods were conducted in sets to test the accuracy of the error predictions and to compare the performance of the methods for a wide variety of noise levels, missing measurements, and biased measurements.

The first set of trials was used to test the validity of the error prediction, and indirectly, the assumption that angular orientation and velocity measurement errors can be considered negligible compared to the acceleration errors. Fifty (50) ensembles of data were produced with each channel of force plate noise set at a standard deviation of 0.1 N (N-m in the case of

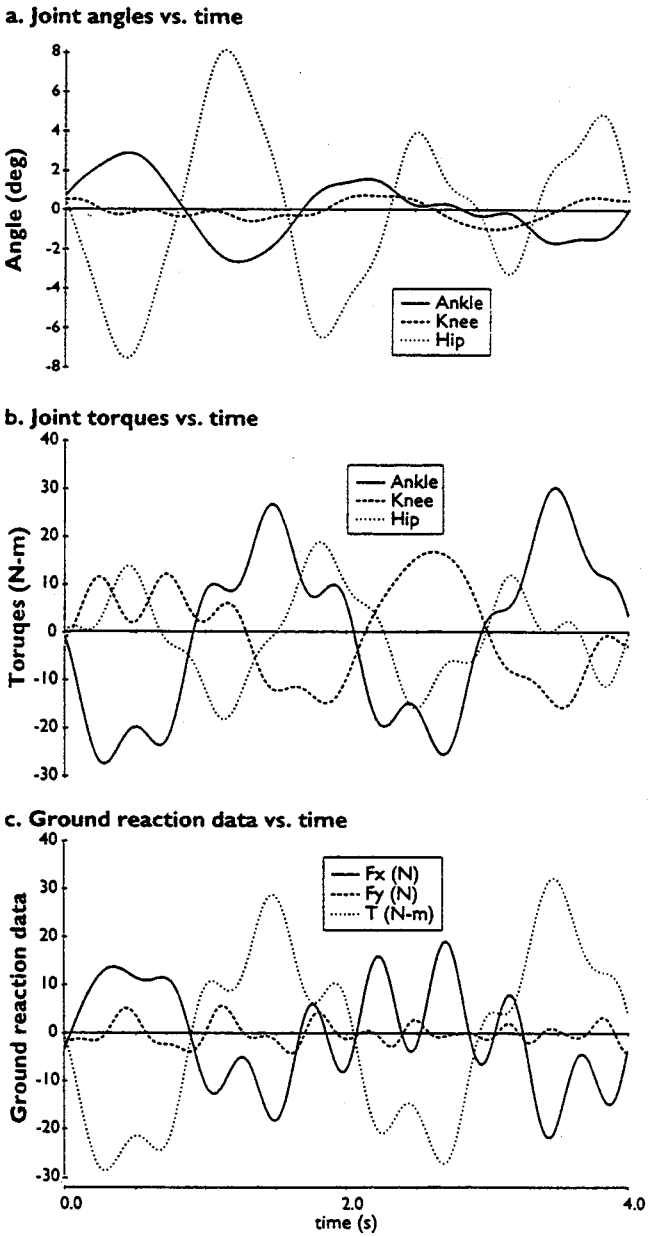

Fig. 2 Benchmark simulation of postural movement: (*a*) Joint angles versus time for ankle, knee, hip. (*b*) Joint torques versus time. (*c*) Ground reaction data, for horizontal force (F_x), vertical force (F_y), and ground reaction torque (T).

torque) and marker position noise at 1 cm (both horizontal and vertical). The square root of the ensemble-averaged square error was calculated across time, and compared with the predicted values given by the square roots of the diagonal elements of the covariance matrix.

The second set of trials was used to compare the performance of the static optimization and conventional methods for a wide range of noise variations. The standard deviation of noise on each of the force measurements was set at values ranging from 0.001 N (0.001 N-m in the case of ground reaction torque) to 10 N (1 N-m for ground reaction torque) in increments of a factor of 10, and the position measurements at values ranging from 0.01 cm to 3.2 cm, also in increments of half orders of magnitude. One ensemble was computed for each combination of noise levels, and the errors were summarized using the square root of the *time-averaged* square error,

$$\text{RMSE}i = \sqrt{\frac{1}{N} \sum_{k=1}^{N} (\tau_i[k] - (\bar{\tau}_i[k])^2} \tag{14}$$

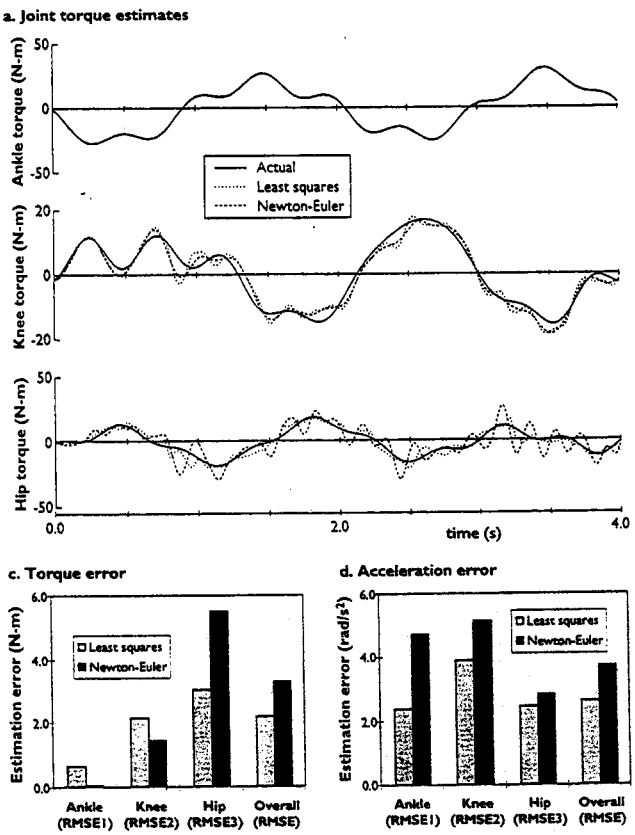

Fig. 3 Comparison of results from benchmark test of Newton–Euler and least-squares methods. Least-squares method substantially improves estimates for joints distal to force plate, resulting in lower overall error. (*a*) Joint torque estimates over time, versus actual torques at ankle, knee, and hip. (*b*) Joint torque estimation error, averaged over time, for each joint and overall error (RMSE). (*c*) Joint angular acceleration estimation errors, averaged over time, are reduced using least-squares method for all joints.

calculated for each joint, and with an overall measure for all joints taken to be the magnitude of the torque error vector summarized in a similar manner:

$$\mathrm{RMSE} = \sqrt{\frac{1}{N}\sum_{k=1}^{N} \|\tau[k] - \bar{\tau}[k]\|^2}\,. \qquad (15)$$

The third set of trials was used to compare performance of the methods with missing reaction force data. RMSE was calculated with measurement noise set at the same values as used in the first set, for every possible combination of missing force plate data. One ensemble was calculated for each combination.

The final set of simulations was used to compare performance for varying amounts of bias in the force plate measurements. The bias in this case consisted of misalignment of the force plate and motion analysis coordinate systems by amounts varying from 0 to 1 cm in steps of 0.1 cm. Measurement noise remained at 1 cm for marker positions, 0.1 N for forces (0.1 N-m for ground reaction torque). The RMSE was calculated for a single ensemble of each of these cases.

Results

Overall time-averaged torque and acceleration errors were computed for both methods, as shown in Fig. 3. For measurement noise standard deviations of 1 cm for marker position and 0.1 N (horizontal and vertical reaction force) and 0.1 N-m (ground reaction torque) for force measurements, the Newton–Euler method produced more precise estimates of ankle and knee torques. The ankle torque was especially precise with an error of 0.043 N-m, compared to 0.61 N-m (RMSE1) using the least-squares method. However, the advantage is reduced for knee torque, 1.43 N-m compared to 2.13 N-m (RMSE2), and disappears at the hip, 5.49 N-m compared to 3.02 N-m (RMSE3). This dramatic difference in hip torque makes the least-squares method advantageous overall, with an RMSE 34 percent (2.16 N-m versus 3.27 N-m) lower than that using the Newton–Euler method. Although the conventional method produced better results for joints closest to the force plate, this precision came at the expense of much larger errors at the hip, and a residual torque of 51.3 N-m (RMSE4). If this residual were to be included in overall RMSE, the reduction gained by using the least-squares method would increase to approximately 95 percent. The least-squares method also resulted in substantial reductions in error in the joint angular acceleration estimates, with overall error (RMSE) reduced by 30 percent (3.72 to 2.60 rad/s^2).

The results for the ensemble-averaged trials are shown in Fig. 4. Predicted and actual standard error are given for each joint torque over time using both Newton–Euler and least-squares methods (Fig. 4(*a*)), and for each joint angular acceleration over time using only the least-squares method (Fig. 4(*b*)). Predicted standard error was derived from the predicted covariances of Eqs. (12) and (13). The predictions show that, for the selected noise levels, the least-squares method should theoretically outperform the conventional inverse dynamics method where all measurements are available. This advantage should be greatest for the joint most distal to the force plate, where the error is predicted to be reduced by about 30 percent. While the simulations show that the predictions tend to underestimate the error, they nevertheless affirm that the least-squares method outperforms the Newton–Euler method. The poor precision of the prediction was thought to stem in part from noise in angular orientations and velocities, which are not taken into account by the model. To test this possibility, the ensembles were recomputed with the same measurement noise levels on f_0 and $\ddot{\phi}$, but with $\phi' = \bar{\phi}$ and $\dot{\phi}' = \bar{\dot{\phi}}$. The results, shown in Fig. 4(*c*), show that the ensemble errors are much closer to their predicted values, verifying that angular orientation and velocity errors adversely affect predictions of overall error.

Comparisons for a variety of motion data and force plate noise levels show that the proposed method was more precise for a variety of situations. A graph of absolute joint torque estimate errors (RMSE, see Fig. 5(*a*)) shows that error magnitude generally increases with both marker and force measurement noise magnitude using both methods. However, in all of these cases, the least-squares estimate was more precise, with a relative reduction in RMSE (Fig. 5(*b*)) ranging from 20 to 60 percent for 48 out of the 56 combinations used, with a median reduction of approximately 35 percent. These ranges demonstrate that precision may be improved for a wide range of noise levels, measurement techniques, and differentiation methods.

Errors in joint torque estimates (RMSE) with varying force plate offsets are compared in Fig. 6. For every case in which at least one force plate measurement was available, the least-squares method produced more precise estimates; when only acceleration measurements are available, the system is determinate and the two methods are equivalent. There were three cases in which the proposed method outperformed the Newton–Euler method by a factor of four or more: when horizontal ground reaction force and ground reaction torque (91 percent reduction in RMSE) were available, horizontal and vertical forces alone (78 percent), reaction torque alone (90 percent), and horizontal force alone (76 percent).

Errors for the case when all force measurements are available, but with a horizontal bias in alignment with the motion data coordinate system, are compared in Fig. 7. Using the Newton–

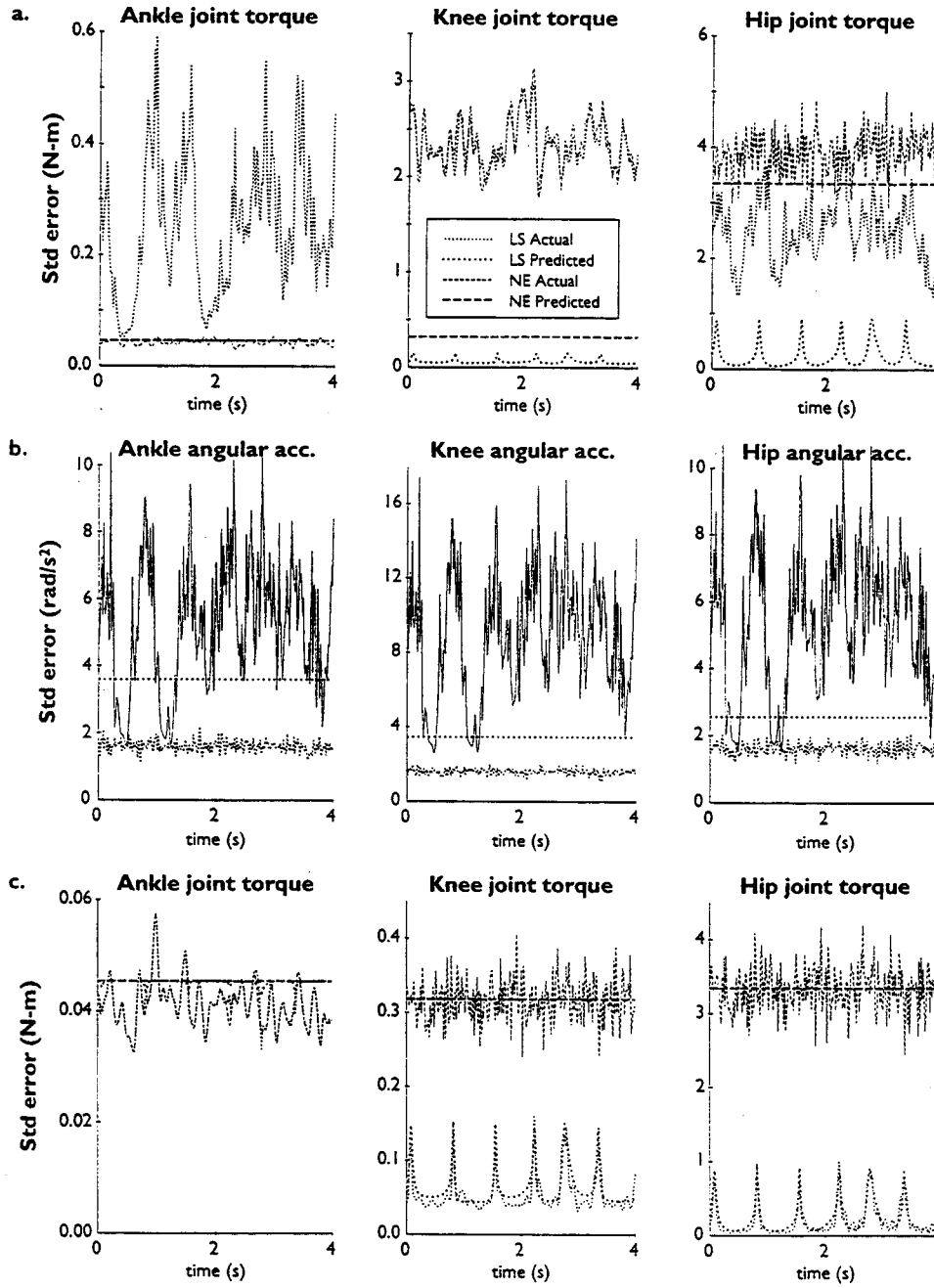

Fig. 4 Ensemble-averaged standard errors over time, for Newton–Euler (NE) and Least-Squares (LS) methods applied to benchmark system. Errors are shown in three columns, corresponding to the ankle, knee, and hip joints. LS results are denoted by a dotted line, and NE by a dashed line. Actual standard errors are denoted by a thin line, and predicted values by a thicker line. (*a*) Actual and predicted standard errors of joint torque estimates. Noise in angular orientation and velocity measurements causes predictions to underestimate actual error. (For ankle torque, NE and LS predictions are nearly identical.) (*b*) Actual and predicted standard errors of joint angular acceleration estimates. Measured accelerations, found by double-differentiating filtered angular orientation measurements, are denoted by a solid line. NE method does not estimate accelerations, but assumes they are equal to the measured values. Acceleration error predictions are also underestimated. (*c*) Joint torque errors computed using exact angular orientations and velocities, but noisy accelerations, result in much better predictions. Motion analysis precision therefore determines accuracy of error prediction.

Euler inverse dynamics method, the overall RMSE increased linearly with bias. With a misalignment of 1 cm, the error increases from 3.27 N-m to 7.52 N-m RMSE, a factor of 2.3. In contrast, the static optimization is unaffected by bias, with error remaining constant at 2.17 N-m RMSE. The relative reduction in error increases from 34 to 71 percent when the bias reaches 1 cm.

Discussion

For a wide range of noise levels, the least-squares method produces smaller overall torque errors than the Newton–Euler method. However, the conventional method often provides better estimates for the joints closest to the force plate (see Fig. 3). This comes at the expense of much poorer precision at the other joints, and the production of residual torques and forces at the

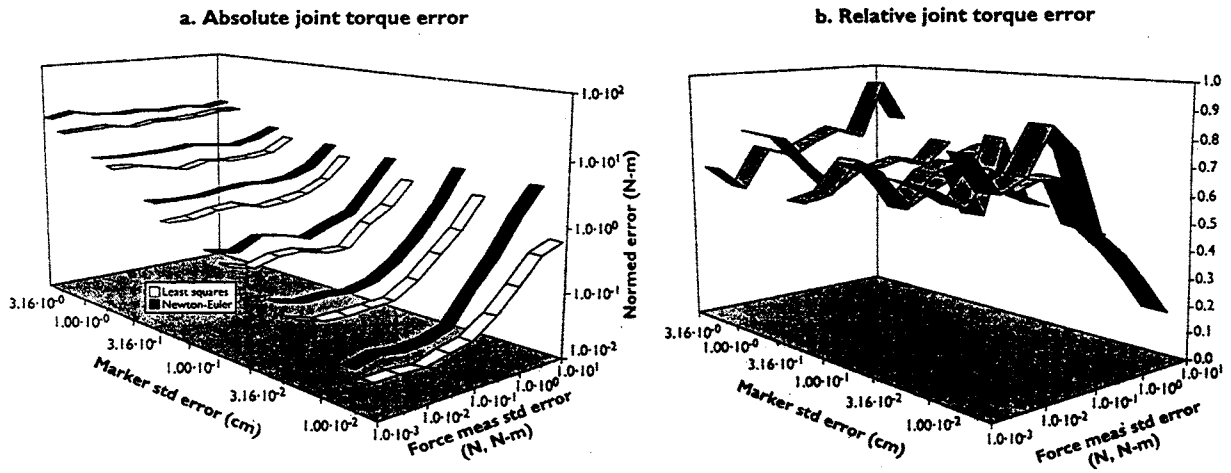

Fig. 5 Comparison of joint torque estimation errors for varying levels of noise in forces and marker measurements: (*a*) Absolute errors (RMSE) for Newton–Euler and least-squares methods. (*b*) Relative errors, least-squares RMSE as a fraction of Newton–Euler RMSE. Least-squares method resulted in reduced error for every combination of noise levels, with a median reduction of 30 percent.

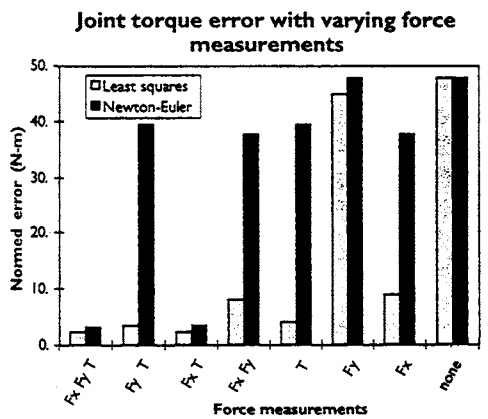

Fig. 6 Comparison of joint torque estimation error (RMSE) for both methods, with varying number of force plate measurements. All possible combinations of force measurements were tested, using all acceleration measurements for each case. The force measurements used are denoted by F_x for horizontal ground reaction force, F_y for vertical force, and T for ground reaction torque. Least-squares method results in substantially reduced error even when some force measurements are not included.

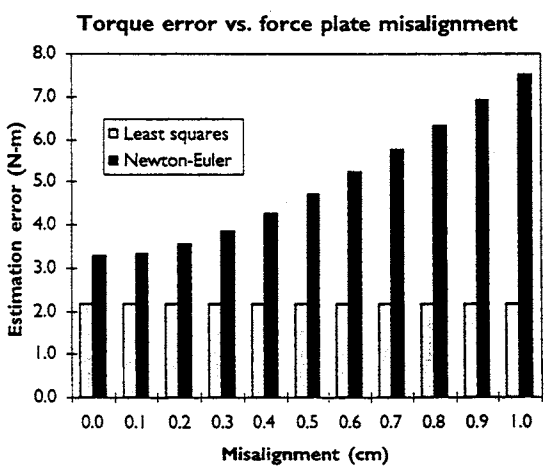

Fig. 7 Comparison of joint torque estimation error (RMSE) for both methods, with varying amounts of bias due to misalignment between force plate and motion measurement coordinate systems. Least-squares method successfully eliminates effects of bias.

upper end of the system. In contrast, the least-squares method performs better on these same joints distal to the force plate, where absolute errors are usually far greater, and produces no residual torques at the top-most segment. In terms of overall RMSE, the proposed method provided better estimates for every combination of noise levels (Fig. 5), showing that these results are not particular to an ideal test case. Moreover, the proposed method can also provide minimum mean-square error estimates of the angular acceleration and ground reaction force measurements.

One major requirement is that measurement covariances are required. These quantities can be estimated roughly by examining measurement data after low-pass filtering and (if appropriate) numerical differentiation. It is also possible to compute the covariances theoretically from knowledge of the precision of measurement equipment and by modeling the data processing, as described in Appendix B. It is, however, difficult to account for other sources of noise such as motion of the markers on the skin or vibration of the force plate, or to describe non-white, non-Gaussian noise. Fortunately, these concerns are somewhat alleviated by the observation that least-squares methods of this sort are generally quite robust. For the test case described above, variations of a single covariance value by 100 percent produced a mean change in torque errors of only 7 percent. In fact, another test showed that when all of the covariances were arbitrarily set equal to each other, the least-squares method still outperformed the conventional method for all but two of the 54 combinations of noise levels tested (as in Fig. 6).

There remains nevertheless a compelling reason for accurately estimating measurement covariance: to facilitate prediction of the estimation error. The results show that Eqs. (12) and (13) can be used to predict the estimation error covariance as long as reasonable estimates of measurement noise covariance are available and angular orientation and velocity measurements are fairly precise (see Fig. 4(*c*)). When these last measurements are imprecise, however, the actual error may be several times higher than predicted (see Fig. 4(*a*)). Even in such cases, the covariance predictions may be useful for three purposes. First, they may still predict the relative changes in estimation error that occur across time (i.e., as the body changes configuration). Second, they are useful for predicting theoretically the amount by which precision can be improved by using the proposed least-squares techniques. Third, the fact that error covariance is reduced, even though by an amount smaller than predicted (see Fig. 5), shows that the errors in angular acceleration and force measurements are dominant, as hypothesized. Although errors in angular orientation and velocity adversely

affect the results, the least-squares method still provides better precision.

The robustness of the least-squares formulation is demonstrated by its performance when some force measurements are missing. While error increased with loss of measurement data regardless of method, the static optimization method outperformed the conventional method in every case, and in relative terms usually experienced a smaller increase in error. In fact, when horizontal ground reaction forces were removed, the proposed method's estimates had only 7 percent greater joint torque error than the standard method's estimates using all measurements. This robustness indicates that the proposed method is especially useful when some data are missing or when measurements are especially noisy. There may in fact be cases when a measurement such as horizontal ground reaction force may be intentionally discarded to save on equipment expense. The prediction of error covariance can be used to evaluate when such a situation is warranted.

This robustness stems from the formulation's flexibility. It can make use of any number of measurements, as long as they are sufficient to make the problem determinate. Beyond that minimum, precision increases with the number of measurements, as long as they can be included in equations that are linear in the estimation variables. For example, accelerometer measurements are related to the joint angular accelerations by a simple coordinate transformation, and could be useful for improving the joint torque estimates at joints far removed from the force plate.

Another example of the flexibility of this formulation is the inclusion of measurement bias. Any constant bias in the measurements can be optimized out of the estimates, as long as they are accounted for in the formulation, and as long as there are enough data to make the problem determinate. Because there are typically many time steps, this second consideration is typically not an issue. And if any calibrations are in doubt, it is not unreasonable to include them as a conservative measure. In fact, their inclusion makes it much less important to deal with issues such as alignment of force plate and measurement coordinate system origins (although their respective axes must nonetheless be parallel each other) or zeroing of force measurements. Moreover, this reformulation of the problem poses little penalty on computation. In fact, using an efficient sparse matrix solver in MATLAB (The Mathworks Inc., Natick, Mass.), the inverse dynamics method actually ran about 6 percent *faster* using the sparse formulation.

It is theoretically and practically unsurprising that the static optimization method performs well relative to the traditional method. An interesting comparison is between the static optimization method and a dynamic optimization method such as that proposed by Chao and Rim (1973). These methods differ in the fact that the method proposed here utilizes the equations of motion merely as algebraic equations at each point in time, but the dynamic optimization method recognizes their true utility as differential equations, which place constraints over time. Dynamic optimization therefore recognizes physical limitations on movement over time, and finds the trajectory of joint torques that best matches the measurements both spatially and temporally. Theoretically it is the better method, and can achieve high levels of precision depending on the choice of optimization parameters, but the difficulties mentioned in the introduction make dynamic optimization a poor choice in practice.

The least-squares method would therefore appear to be ideal for many applications. It does, however, have one major disadvantage. Implementation requires the formulation of equations of motion for the system, and equations relating ground reaction forces and joint torques, which are both more difficult than simple iteration of the Newton–Euler equations for each segment. Traditionally, such formulations have required advanced knowledge of multi-body dynamics (Greenwood, 1988). However, these equations may also be solved symbolically using commercial software packages or numerically using kinematic constraints, as described in Appendix A. Nonetheless, traditional methods remain useful, particularly when simplicity is desired, and when measurements do not suffer from excessive noise.

Finally, it is important to note that any method mentioned here is subject to systematic errors that affect accuracy. Systematic errors may be produced by inadvertant filtering of useful data along with the noise, by poor placement of body markers, and by inaccurate estimation of body segment dimensional and inertial parameters. The proposed method addresses none of these issues, and seeks only to improve *precision* by reducing the effects of random noise. The overall *accuracy*, on the other hand, depends on many other factors and is a much more difficult issue to address.

Acknowledgments

This work was supported in part by a grant from the Whitaker Foundation, NSF Grant IBN-9511814, NIH Grant P60DC02072-03, and the Claude Pepper Older Americans Independence Center at the University of Michigan.

References

Chao, E. Y., and Rim, K., 1973, "Application of Optimization Principles in Determining the Applied Moments in Human Leg Joints During Gait," *Journal of Biomechanics*, Vol. 6, pp. 497–510.

Golub, G. H., and Van Loan, C. F., 1989, *Matrix Computations*, Johns Hopkins University Press, Baltimore, MD.

Greenwood, D. T., 1988, *Principles of Dynamics*, Prentice-Hall, Englewood Cliffs, NJ.

Kane, T. R., and Levinson, D. A., 1985, *Dynamics, Theory and Applications*, McGraw-Hill, New York.

Kuo, A. D., 1994, "A Smoothing Method for Computing Inverse Dynamics," *World Congress of Biomechanics Abstracts*, Amsterdam, The Netherlands.

Kuo, A. D., 1995, "A Simple Method of Improving Precision of Inverse Dynamics Computations," *Proc. 18th Annual Meeting of the American Society of Biomechanics*, Stanford, CA.

McCaw, S. T., and DeVita, P., 1995, "Errors in Alignment of Center of Pressure and Foot Coordinates Affect Predicted Lower Extremity Torques," *Journal of Biomechanics*, Vol. 28, pp. 985–988.

Stark, H., and Woods, J. W., 1986, *Probability, Random Processes, and Estimation Theory for Engineers*, Prentice-Hall, Englewood Cliffs, NJ.

Strang, G., 1988, *Linear Algebra and its Applications*, Harcourt, Brace, Jovanovich, San Diego, CA.

Vaughan, C. L., Andrews, J. G., and Hay, J. G., 1982, "Selection of Body Segment Parameters by Optimization Methods," ASME JOURNAL OF BIOMECHANICAL ENGINEERING, Vol. 104, pp. 38–44.

Winter, D. A., 1990, *Biomechanics and Motor Control of Human Movement*, Wiley-Interscience, New York.

APPENDIX A

Equations for Four-Segment Model

This appendix provides the equations of motion for the four-segment system used as a benchmark. Both equations of motion (3) and the ground reaction force Eq. (4) are derived using Newton–Euler equations for rigid-body motion and simple kinematics. They have the advantage of being solvable either symbolically or numerically. The symbolic solution is exactly equivalent to the equations found by more advanced methods such as that of Lagrange (Greenwood, 1988) or Kane (Kane and Levinson, 1985). The numerical solution requires no algebraic reduction (by eliminating constraints numerically) and is easy to implement in software. This method can easily be extended for more segments or to three dimensions as noted in Appendix C.

In order to derive Eqs. (3) and (4), it is advantageous first to derive the equations of motion for the four-segment system with no constraint on rotation of segment 1. The result is a superset of the equations of motion with segment 1 held static, and the extra degree of freedom is used to solve for the ground reaction torque. To facilitate the derivation, the following

stacked vectors are defined for angular orientations, joint torques, segment center of mass positions, and reaction forces:

$$\Phi \equiv \begin{bmatrix} \phi_1 \\ \phi_2 \\ \vdots \\ \phi_n \end{bmatrix} = \begin{bmatrix} \phi_1 \\ \phi \end{bmatrix}, \quad T \equiv \begin{bmatrix} \tau_0 \\ \tau_1 \\ \vdots \\ \tau_{n-1} \end{bmatrix} = \begin{bmatrix} \tau_0 \\ \tau \end{bmatrix},$$

$$x_c \equiv \begin{bmatrix} x_{c1} \\ x_{c2} \\ \vdots \\ x_{cn} \end{bmatrix}, \quad f \equiv \begin{bmatrix} f_0 \\ f_1 \\ \vdots \\ f_{n-1} \end{bmatrix}$$

The equations of motion are found by eliminating kinematic constraints from the Newton–Euler equations. The kinematic constraints are those relating the position and orientation of the segments. These constraints are expressed here as the center of mass positions of the segments as a vector function of the generalized coordinates, which in this system, are the segment angles:

$$x_c = \begin{bmatrix} l_{c1}c_1 \\ l_{c1}s_1 \\ l_1c_1 + l_{c2}c_2 \\ l_1s_1 + l_{c2}s_2 \\ l_1c_1 + l_2c_2 + l_{c3}c_3 \\ l_1s_1 + l_2s_2 + l_{c3}s_3 \\ l_1c_1 + l_2c_2 + l_3c_3 + l_{c4}c_4 \\ l_1s_1 + l_2s_2 + l_3c_3 + l_{c4}s_4 \end{bmatrix}, \tag{A1}$$

where $s_i \equiv \sin \phi_i$, $c_i \equiv \cos \phi_i$, l_i is the length of segment i, and l_{ci} is the distance from the end of segment i most proximal to the ground to its center of mass (see Fig. 1).

The first and second time derivatives of Eq. (A1) may be written in matrix form by defining the Jacobian and its derivative,

$$J \equiv \frac{\partial x_c}{\partial \Phi}, \quad J = \begin{bmatrix} -l_{c0}s_0 & 0 & 0 & 0 \\ l_{c1}c_1 & 0 & 0 & 0 \\ -l_1s_1 & -l_{c2}s_2 & 0 & 0 \\ l_1c_1 & l_{c2}c_2 & 0 & 0 \\ -l_1s_1 & -l_2s_2 & -l_{c3}s_3 & 0 \\ l_1c_1 & l_2c_2 & l_{c3}c_3 & 0 \\ -l_1s_1 & -l_2s_2 & -l_3s_3 & -l_{c4}s_4 \\ l_1c_1 & l_2c_2 & l_3c_3 & l_{c4}c_4 \end{bmatrix},$$

$$\dot{J} = \begin{bmatrix} -l_{c1}c_1\dot{\phi}_1 & 0 & 0 & 0 \\ -l_{c1}s_1\dot{\phi}_1 & 0 & 0 & 0 \\ -l_1c_1\dot{\phi}_1 & -l_{c2}c_2\dot{\phi}_2 & 0 & 0 \\ -l_1s_1\dot{\phi}_1 & -l_{c2}s_2\dot{\phi}_2 & 0 & 0 \\ -l_1c_1\dot{\phi}_1 & -l_2c_2\dot{\phi}_2 & -l_{c3}c_3\dot{\phi}_3 & 0 \\ -l_1s_1\dot{\phi}_1 & -l_2s_2\dot{\phi}_2 & -l_{c3}s_3\dot{\phi}_3 & 0 \\ -l_1c_1\dot{\phi}_1 & -l_2c_2\dot{\phi}_2 & -l_3c_3\dot{\phi}_3 & -l_{c4}c_4\dot{\phi}_4 \\ -l_1s_1\dot{\phi}_1 & -l_2s_2\dot{\phi}_2 & -l_3s_3\dot{\phi}_3 & -l_{c4}s_4\dot{\phi}_4 \end{bmatrix}$$

so that

$$\dot{x}_c = J\dot{\Phi} \tag{A2}$$

$$\ddot{x}_c = J\ddot{\Phi} + \dot{J}\dot{\Phi}. \tag{A3}$$

Summing the forces acting on each segment and combining them in vector form, Newton's equation for rigid-body motion can be written as

$$S_2 \cdot f = M_D \cdot \ddot{x}_c + g_V \tag{A4}$$

where the following additional quantities are defined:

$$S_2 \equiv \begin{bmatrix} I^{2\times2} & -I^{2\times2} & & \\ & I^{2\times2} & -I^{2\times2} & \\ & & I^{2\times2} & -I^{2\times2} \\ & & & I^{2\times2} \end{bmatrix}$$

$$M_D \equiv \text{diag}\,(m_1, m_1, m_2, m_2, m_3, m_3, m_4, m_4)$$
$$g_V \equiv [0 \quad m_1 \quad 0 \quad m_2 \quad 0 \quad m_3 \quad 0 \quad m_4]^T g$$

with $I^{2\times2}$ denoting the 2-by-2 identity matrix, and g denoting the gravitational constant.

Similarly, Euler's equation for rigid-body rotation can be written as

$$I\ddot{\Phi} = S_1 \cdot \mathcal{T} + P \cdot f \tag{A5}$$

where I is the diagonal matrix of segment moments of inertia $I \equiv \text{diag}\,(I_1, I_2, I_3, I_4)$, and

$$S_1 \equiv \begin{bmatrix} 1 & -1 & & \\ & 1 & -1 & \\ & & 1 & -1 \\ & & & 1 \end{bmatrix}$$

$$P \equiv \begin{bmatrix} l_{c1}s_1 & -l_{c1}c_1 & (l_1 - l_{c1})s_1 & -(l_1 - l_{c1})c_1 & 0 & 0 & 0 & 0 \\ 0 & 0 & l_{c2}s_2 & -l_{c2}c_2 & (l_2 - l_{c2})s_2 & -(l_2 - l_{c2})c_2 & 0 & 0 \\ 0 & 0 & 0 & 0 & l_{c3}s_3 & -l_{c3}c_3 & (l_3 - l_{c3})s_3 & -(l_3 - l_{c3})c_3 \\ 0 & 0 & 0 & 0 & 0 & 0 & l_{c4}s_4 & -l_{c4}c_4 \end{bmatrix}$$

The forces f may be eliminated by substituting Eqs. (A3) and (A4) into Eq. (A5):

$$I\ddot{\Phi} = S_1 \cdot \mathcal{T} + P \cdot (S_2^{-1} \cdot M_D \cdot J\ddot{\Phi} + S_2^{-1} \cdot M_D \cdot \dot{J}\dot{\Phi} + S_2^{-1} \cdot g_V) \tag{A6}$$

which may be rearranged as

$$\mathcal{M}\ddot{\Phi} = S_1 \cdot \mathcal{T} + \mathcal{V} + \mathcal{G} \tag{A7}$$

given the definitions

$$\mathcal{M} \equiv I - P \cdot S_2^{-1} \cdot M_D \cdot J$$

$$\mathcal{V} \equiv P \cdot S_2^{-1} \cdot M_D \cdot \dot{J}\dot{\Phi}$$

$$\mathcal{G} \equiv P \cdot S_2^{-1} \cdot g_V.$$

It is instructive to note that Eq. (A7) may be partitioned into an equation for the motionless segment 0; and the equations of motion for the remaining segments, Eq. (3):

$$\begin{bmatrix} m_{11} & m_{12} & m_{13} & m_{14} \\ m_{12} & & & \\ m_{13} & & M(\phi) & \\ m_{14} & & & \end{bmatrix} \cdot \begin{bmatrix} 0 \\ \ddot{\phi} \end{bmatrix} = \begin{bmatrix} \tau_0 - \tau_1 \\ Q \cdot \tau \end{bmatrix} \begin{bmatrix} \mathcal{V}_1 \\ v(\phi, \dot{\phi}) \end{bmatrix} + \begin{bmatrix} \mathcal{G}_1 \\ g(\phi) \end{bmatrix} \tag{A8}$$

The ground reaction forces may be found from Eq. (A4),

$$f_0 = S_2^l \cdot M_D \cdot \ddot{x} + S_2^l \cdot g_V \tag{A9}$$

where $S_2^l \equiv [I^{2\times2}\ I^{2\times2}\ I^{2\times2}\ I^{2\times2}]$ is the first (block) row of the inverse of S_2. Similarly, the ground reaction torque may be found from Eq. (A7) to be

$$\tau_0 = S_1^l \cdot \mathcal{M}\ddot{\Phi} - \mathcal{V}_1 - \mathcal{G}_1 \tag{A10}$$

where S_1^l is the first row of the inverse of S_1. The following definitions then yield Eq. (4):

$$C(\phi) \equiv \begin{bmatrix} S_1^l \cdot \mathcal{M} \\ S_2^l \cdot M_D \cdot J \end{bmatrix},\ c(\phi, \dot{\phi}) \equiv \begin{bmatrix} V_1 + G_1 \\ -S_2^l M_D \dot{J}\dot{\Phi} + S_2^l g_V \end{bmatrix}.$$

These same equations given above may be used to derive the matrix F used in Eq. (12), with a few modifications. Equations (A4) and (A5) are rewritten to separate the ground reaction measurements f_0 and τ_0, and an extra degree of freedom is added to allow for a residual, τ_n. This is accomplished by defining

$$\hat{\mathcal{T}} \equiv \begin{bmatrix} \tau_1 \\ \tau_2 \\ \vdots \\ \tau_n \end{bmatrix},\ \hat{f} \equiv \begin{bmatrix} f_1 \\ f_2 \\ \vdots \\ f_n \end{bmatrix},\ \hat{S}_1 \equiv \begin{bmatrix} -1 & & & \\ 1 & -1 & & \\ & 1 & -1 & \\ & & 1 & -1 \end{bmatrix},$$

$$\hat{S}_2 \equiv \begin{bmatrix} -I^{2\times2} & & & \\ I^{2\times2} & -I^{2\times2} & & \\ & I^{2\times2} & -I^{2\times2} & \\ & & I^{2\times2} & -I^{2\times2} \end{bmatrix},$$

$$P_0 \equiv \begin{bmatrix} l_{c1}s_1 & -l_{c1}c_1 \\ 0 & 0 \\ 0 & 0 \\ 0 & 0 \end{bmatrix}$$

$$\hat{P} \equiv \begin{bmatrix} (l_1 - l_{c1})s_1 & -(l_1 - l_{c1})c_1 & 0 & 0 \\ l_{c2}s_2 & -l_{c2}c_2 & (l_2 - l_{c2})s_2 & -(l_2 - l_{c2})c_2 \\ 0 & 0 & l_{c3}s_3 & -l_{c3}c_3 \\ 0 & 0 & 0 & 0 \end{bmatrix}$$

which are used to rearrange Eqs. (A4) and (A5) into

$$\hat{f} = \hat{S}_2^{-1}\{M_D \cdot \ddot{x}_c + g_V\} - (S_2^l)^T f_0 \tag{A11}$$

$$\hat{\mathcal{T}} = \hat{S}_1^{-1}\{I\ddot{\Phi} - \hat{P} \cdot \hat{f} - P_0 \cdot f_0\} + (S_1^l)^T \cdot \tau_0. \tag{A12}$$

The output of the Newton–Euler method is $\mathcal{T}'$, found by combining Eqs. (A3), (A11), and (A12):

$$\hat{\mathcal{T}} = \hat{S}_1^{-1}\{I\ddot{\Phi} - \hat{P} \cdot \hat{S}_2^{-1}\{M_D \cdot (J\ddot{\Phi} + \dot{J}\dot{\Phi}) + g_V\} + \{\hat{P} \cdot (S_2^l)^T - P_0\} f_0\} + (S_1^l)^T \cdot \tau_0, \tag{A13}$$

so that

$$\hat{\mathcal{T}} = [\hat{S}_1^{-1}(I - \hat{P}\hat{S}_2^{-1}M_D J)\quad (S_1^l)^T\quad \hat{S}_1^{-1}\{\hat{P} \cdot (S_2^l)^T - P_0\}] \cdot \begin{bmatrix} \ddot{\Phi} \\ \tau_0 \\ f_0 \end{bmatrix} - \hat{S}_1^{-1}\hat{P}\hat{S}_2^{-1}(M_D \dot{J}\dot{\Phi} + g_V). \tag{A14}$$

Equation (11) is then found by substituting the measured quantities into Eq. (A14), and F is therefore equal to the first block matrix above, with the first row removed because $\ddot{\phi}_1 = 0$.

For completeness, the actual equations of motion Eq. (A8) and the associated parameters are given below:

$$b_1 \equiv m_1 l_{c1} + (m_2 + m_3 + m_4) l_1$$
$$b_2 \equiv m_2 l_{c2} + (m_3 + m_4) l_2$$
$$b_3 \equiv m_3 l_{c3} + m_4 l_3$$
$$b_4 \equiv m_4 l_{c4}$$
$$a_{11} \equiv I_1 + m_1 l_{c1}^2 + (m_2 + m_3 + m_4) l_1^2$$
$$a_{12} \equiv b_2 l_1$$
$$a_{13} \equiv b_3 l_1$$
$$a_{14} \equiv b_4 l_1$$
$$a_{22} \equiv I_2 + m_2 l_{c2}^2 + (m_3 + m_4) l_2^2$$
$$a_{23} \equiv b_3 l_2$$
$$a_{24} \equiv b_4 l_2$$
$$a_{33} \equiv I_3 + m_3 l_{c3}^2 + m_4 l_3^2$$
$$a_{34} \equiv b_4 l_3$$
$$a_{44} \equiv I_4 + m_4 l_{c4}^2$$

These constants are used in the terms of Eq. (A7):

$$\mathcal{M}(\Phi) = \begin{bmatrix} a_{11} & a_{12}c_{12} & a_{13}c_{13} & a_{14}c_{14} \\ a_{12}c_{12} & a_{22} & a_{23}c_{23} & a_{24}c_{24} \\ a_{13}c_{13} & a_{23}c_{23} & a_{33} & a_{34}c_{34} \\ a_{14}c_{14} & a_{24}c_{24} & a_{34}c_{34} & a_{44} \end{bmatrix}$$

$$\mathcal{V}(\Phi, \dot{\Phi}) = \begin{bmatrix} 0 & -a_{12}s_{12}\dot{\phi}_2 & -a_{13}s_{13}\dot{\phi}_3 & -a_{14}s_{14}\dot{\phi}_4 \\ a_{12}s_{12}\dot{\phi}_1 & 0 & -a_{23}c_{23}\dot{\phi}_3 & -a_{24}s_{24}\dot{\phi}_4 \\ a_{13}s_{13}\dot{\phi}_1 & a_{23}s_{23}\dot{\phi}_2 & 0 & -a_{34}s_{34}\dot{\phi}_4 \\ a_{14}s_{14}\dot{\phi}_1 & a_{24}s_{24}\dot{\phi}_2 & a_{34}s_{34}\dot{\phi}_3 & 0 \end{bmatrix} \cdot \begin{bmatrix} \dot{\phi}_1 \\ \dot{\phi}_2 \\ \dot{\phi}_3 \\ \dot{\phi}_4 \end{bmatrix}$$

$$\begin{bmatrix} 0 & 0 & 0 & 0 \\ 0 & 0 & 0 & 0 \\ (l_3 - l_{c3})s_3 & -(l_3 - l_{c3})c_3 & 0 & 0 \\ l_{c4}s_4 & -l_{c4}c_4 & (l_4 - l_{c4})s_4 & -(l_4 - l_{c4})c_4 \end{bmatrix}$$

$$\mathcal{G}(\Phi) = [-b_1 c_1\quad -b_2 c_2\quad -b_3 c_3\quad -b_4 c_4]^T \cdot g$$

These parameter values were used for the benchmark problem:

$l_1 = 0.177$ m, $l_2 = 0.405$ m, $l_3 = 0.440$ m, $l_4 = 0.795$ m

$l_{c1} = 0.086$ m, $l_{c2} = 0.235$ m, $l_{c3} = 0.268$ m, $l_{c4} = 0.302$ m

$m_1 = 1.78$ kg, $m_2 = 7.30$ kg $m_3 = 15.5$ kg, $m_4 = 44.6$ kg

$I_1 = 0.0080\ \mathrm{kg \cdot m^2}$, $I_2 = 0.097\ \mathrm{kg \cdot m^2}$,

$I_3 = 0.253\ \mathrm{kg \cdot m^2}$, $I_4 = 1.51\ \mathrm{kg \cdot m^2}$

APPENDIX B

Prediction of Measurement Noise Covariance

Given certain assumptions regarding the characteristics of measurement noise, it is possible to estimate the propagation of noise by the processes of extraction of angular orientation from marker positions, digital filtering, and numerical differentiation. These estimates are based on the modeling of these processes as affine operations on noisy measurements of the form

$$y = Zx + z \tag{B1}$$

where the estimates y are linear in the measurements x with the

addition of some constant term z. The measurements include additive noise w, which is assumed white with mean 0 and covariance W, i.e., $x = \bar{x} + w$. This assumption implies that the error in y will also have zero mean, and from probability theory, a covariance

$$E[(y - \bar{y})(y - \bar{y})^T] = ZWZ^T. \quad \text{(B2)}$$

Error Covariance From Extraction of Angular Orientation From Marker Positions. The error associated with angular orientations depends on the method of marker placement and on the way in which orientation is specified. For the two-dimensional system described in Appendix A, the markers were placed at the joint centers, and angular orientation for each joint, a scalar, was found from

$$\phi_i = \tan^{-1} \frac{y_i - y_{i-1}}{x_i - x_{i-1}} \quad \text{(B3)}$$

where x_i and y_i are the horizontal and vertical marker positions, respectively, at joint i. Taking partial derivatives of Eq. (B3), the error covariance of ϕ, W_ϕ, is found to be

$$W_\phi = E[(\phi - \bar{\phi})(\phi - \bar{\phi})^T] = \begin{bmatrix} 2/l_2 & & & \\ & 2/l_3 & & \\ & & \ddots & \\ & & & 2/l_n \end{bmatrix} W_x \quad \text{(B4)}$$

where l_i is the length of segment i, and W_x is the scalar variance in marker position.

Error Covariance Due to Digital Filtering. Low-pass filtering reduces, but does not eliminate, noise in the measurements. Assuming that the filter does not appreciably degrade the desired signal, it is possible to estimate the variance of filter-induced error by evaluating the output variance of the filter driven by noise alone. If the noise w is a scalar white noise random sequence with zero mean and variance W, it has autocorrelation $R_{ww}[n] = W \cdot \delta[0]$ and a corresponding power spectrum $S_{ww}(e^{j\omega}) = W$. The output of a filter with discrete transfer function H driven by this noise has spectrum $S_{w_f w_f} = S_{ww}(e^{j\omega})|H(e^{j\omega})|^2$, where the subscript w_f refers to filtered noise. The variance of this output is given by the autocorrelation of $S_{w_f w_f}$ evaluated at time 0, found by evaluating the integral (Stark and Woods, 1986)

$$W_f = R_{w_f w_f}[0] = \frac{1}{2\pi} \int_{-\pi}^{\pi} S_{xx}(e^{j\omega})|H(e^{j\omega})|^2 d\omega. \quad \text{(B5)}$$

Each measurement channel is filtered independently, so the error covariance is given by a diagonal matrix composed of the individual error variances. Note that the integral in Eq. (B5) cannot generally be given in closed form, and is typically evaluated numerically, depending on the type of filter used. If the desired signal has significant components beyond the bandpass frequency, Eq. (B5) will tend to underestimate the error variance. Such a distortion may be considered a systematic error.

Error Covariance Due to Numerical Differentiation. The process of numerical differentiation produces two types of error. The first is a purely numerical effect due to discretization, which can be estimated using simple numerical analysis. The second is associated with the noise-amplifying nature of time differentiation itself, and can only be estimated given knowledge of the frequency content of both the signal and the measurement noise. The numerical error depends on the differentiation approximation used, and its covariance can be computed given knowledge of the measurement noise covariance. For example, a three-point second derivative of a quantity ϕ is given by

$$\ddot{\phi}[k] = \frac{1}{h^2}(\phi[k+1] - 2\phi[k] + \phi[k-1]) + o(h^2) \quad \text{(B6)}$$

where h is the time step and $o(h^2)$ signifies other terms of order h^2. Since each measurement ϕ is subject to noise, $\phi[k] = \bar{\phi}[k] + w_\phi[k]$, the error covariance of $\ddot{\phi}$ is

$$W_{\ddot{\phi}} = E[(\ddot{\phi} - \bar{\ddot{\phi}})(\ddot{\phi} - \bar{\ddot{\phi}})^T] = \frac{1}{h^4}[1 \quad -2 \quad 1] \cdot \begin{bmatrix} W_\phi & & \\ & W_\phi & \\ & & W_\phi \end{bmatrix} \cdot \begin{bmatrix} 1 \\ -2 \\ 1 \end{bmatrix} = \frac{6}{h^4} W_\phi \quad \text{(B7)}$$

Error Covariance Due to Combined Filtering and Numerical Differentiation. Although measurement noise may reasonably modeled as white noise, the processes of filtering and numerical differentiation both have the effect of coloring this noise. The methods for estimating noise covariance given above are therefore not applicable if the two processes are combined, because the output of one process is the colored input to the other. The error covariance for this case may, however, be estimated by treating both processes as a single filtering operation, that is, by applying Eq. (B5) on a single transfer function $H(e^{j\omega})$, which combines low-pass filtering and numerical differentiation.

APPENDIX C

Inverse Dynamics in Three Dimensions

The proposed method may be formulated for three-dimensional systems with minor changes. There is no conceptual change in the methodology, but the equations must be altered to reflect the three-dimensional nature of the system. The vectors f_i, τ_i, and x_i all become vectors of length 3, and the vector of generalized coordinates ϕ is of length equal to the number of degrees of freedom in the system. (There need not be three rotational degrees of freedom at each joint.) In three dimensions, a segment's angular velocity and angular acceleration are functions of ϕ, $\dot{\phi}$, and $\ddot{\phi}$, which themselves are not generally based on segment angles but on an appropriate three-dimensional coordinate scheme.

The method described in Appendix A may be used by deriving the kinematics for body-centered angular velocity ω_i and acceleration $\dot{\omega}_i$, and then applying the three-dimensional form of Euler's equation:

$$I_i\dot{\omega}_i + \omega_i \times I_i\omega_i = r_i \times f_{i-1} - s_i \times f_i + \tau_{i-1} - \tau_i, \quad \text{(C1)}$$

where I_i are three-by-three inertia tensors. Other matrices and vectors are trivially redefined to reflect changes in size. One significant change is in the redefinition of P as a block matrix:

$$P \equiv \begin{bmatrix} \hat{r}_1 & -\hat{s}_1 & 0 & 0 \\ 0 & \hat{r}_2 & -\hat{s}_2 & 0 \\ 0 & 0 & \ddots & \vdots \\ 0 & 0 & \cdots & r_n \end{bmatrix}$$

where the quantity $\hat{z}$ refers to the matrix

$$\hat{z} \equiv \begin{bmatrix} 0 & -z_3 & z_2 \\ z_3 & 0 & -z_1 \\ -z_2 & z_1 & 0 \end{bmatrix}$$

so that $P \cdot f$ performs the three-dimensional cross products in the right-hand side of Eq. (C1). A similar block matrix using $\hat{\omega}_i$ is used in the left-hand side.